

## Trends in sticking and adsorption of diatomic molecules on the Al(111) surface

A. Hellman, B. Razaznejad, and B. I. Lundqvist

*Department of Applied Physics, Chalmers University of Technology and Göteborg University, SE-412 96 Göteborg, Sweden*

(Received 3 November 2004; revised manuscript received 22 February 2005; published 31 May 2005)

To deepen our understanding of sticking and chemisorption behaviors, a trend study of static and dynamic aspects of the interaction between diatomic molecules, including  $F_2$ ,  $O_2$ ,  $NO$ ,  $CO$ , and  $N_2$ , and the Al(111) surface is performed. General features of free-electron-like metals are extracted and ramifications to other metals are indicated. With a slight generalization of the common form of density-functional theory, potential-energy surfaces (PES's) are calculated for both the adiabatic ground state and some excited states, where one or several electrons have been transferred from the adsorbate to the substrate. One trend applies to chemisorption (from dissociative, over molecular, to absent), and another one to the sticking probability (from unity, over incidence-energy-dependent, to zero). Ground- and excited-state PES's, local densities of states, and estimated electron-transfer probabilities are utilized. Electron transfer and energy dissipation to electron-hole pairs are identified as key processes in the dissociative adsorption. We apply a simple but general sticking model, where the competition between the electron-tunneling and the nuclear-motion time scales plays a central role [Surf. Sci. **532-535**, 126 (2003)], now with a first-principles calculation of excited-state PES's. Measured trends in sticking and chemisorption behaviors are accounted for. Trends can be understood qualitatively in terms of electronegativity, kinetic Pauli-repulsion ranges, bond orders, and asymmetries of the molecules.

DOI: 10.1103/PhysRevB.71.205424

PACS number(s): 82.20.Kh, 82.20.Gk, 68.43.Mn, 68.35.Ja

### I. INTRODUCTION

The understanding of both statics and dynamics of molecule-surface interactions is a key goal in surface science. Such interactions are not only of fundamental importance, they also play essential roles in a large number of technologies, e.g., those based on metal oxidation, heterogeneous catalysis, and thin-film growth. A central process is sticking, often described kinetically but basically a dynamic phenomenon. For instance, it distinguishes surface nobleness from surface reactivity. Gold is one of the noblest metals, inert against all types of oxidation, while potassium is extremely reactive. Sticking of molecules on these surfaces varies very much. Another feature of adsorption is the possibility of a molecularly chemisorbed state. To learn about electronic orbitals involved in the intramolecular bond, the nature of the molecule-surface bond, and any hybridization effect beyond that, experiments like photoemission and scanning-tunneling spectroscopy (STS),<sup>1</sup> in combination with theoretical studies, are very valuable. The importance of sticking and molecular adsorption and the fact that experimental findings on these phenomena might look unsystematic<sup>77</sup> should make an identification of general trends in the molecule-surface interactions valuable. We aim at identifying a few key parameters that describe general trends in the initial sticking. This could improve our ability to prevent or promote adsorption and our understanding of later steps in the gas-surface interaction. This paper is an attempt to do so for the sticking behavior of diatomic molecules on an *sp*-band metal in general, and the Al(111) surface in particular. This should also have implications for noble and transition metals, although here the *d* electrons give very important effects.

Sticking of  $H_2$  on metal surfaces is a model case. It has been addressed in a large number of first-principles studies,<sup>9-17</sup> where the dynamics of the molecule is consid-

ered to occur on the multidimensional adiabatic potential-energy surface (PES), today obtained from density-functional theory (DFT).

The main results can be summarized as follows: The measured sticking probability of  $H_2$  (i) exhibits a normal-energy scaling regardless of strong surface corrugation,<sup>18</sup> (ii) is enhanced by vibrational excitations and steering effects,<sup>15,19</sup> and (iii) is reconciled with results from DFT calculations, based on the adiabatic approximation.<sup>20</sup> A sensitivity to the choice of the energy functional for the exchange and correlation is reported.<sup>11</sup>

On the other hand, the sticking behaviors of some more complex systems seem to call for features beyond the adiabatic DFT calculations. For instance, the initial sticking of  $O_2$  on the Al(111) surface is measured to be low ( $s_0 \sim 10^{-2}$ ) for thermal translational energies and to have a characteristic S-shaped energy dependence.<sup>21-24</sup>

According to conventional accounts for sticking,<sup>25</sup> this indicates the existence of an activation-energy barrier. Adiabatic DFT calculations,<sup>26-30</sup> on the other hand, show no essential activation barrier in the entrance channel of the mapped multidimensional adiabatic PES, implying a sticking probability of unity for all translational energies, according to conventional accounts of sticking. Similar behavior has been reported for  $NO$  on the same surface.<sup>31</sup> An S-shaped energy dependence of the sticking probability is also reported for  $O_2$  on  $Ag(110)$ ,<sup>32</sup> where it increases to a value near unity with increasing translational energy, and on  $Ag(111)$ ,<sup>33</sup> where it remains very low ( $s \sim 10^{-7} - 10^{-3}$ ). In contrast to experimental observations, adiabatic DFT calculations suggest a much higher sticking probability on both of these facets of  $Ag$ .<sup>10,34</sup>

Calculation of the sticking probability calls for dynamical effects, including nonadiabatic ones. This is indicated already for  $H_2$  on metal surfaces<sup>35,36</sup> and certainly anticipated

TABLE I. Schematic overview of published theoretical studies of the sticking of O<sub>2</sub>/Al(111) system.

Source	Ref.	Approach	Energy transfer	Sticking probability	Claims agreement
Yourdshahyan <i>et al.</i>	26,27	Adiabatic	No	Unity, $S=1$	No
Sasaki <i>et al.</i>	28,29	Adiabatic	No	Unity, $S=1$	No
Honkala <i>et al.</i>	30	Adiabatic	No	Unity, $S=1$	No
Ciacchi <i>et al.</i>	38	Adiabatic	No	Unity, $S=1$	No
Hellman <i>et al.</i>	39	Diabatic	Yes	Energy-dependent, $S(E)$	Yes
Katz <i>et al.</i>	41	Diabatic	No	Energy-dependent, $S(E)$	No
Binetti <i>et al.</i>	42,43	Diabatic	No	Energy-dependent, $S(E)$	Yes
Katz <i>et al.</i>					
Behler <i>et al.</i>	44	Adiabatic Diabatic	No	Energy-dependent, $S(E)$	Yes
Present study		Adiabatic Diabatic	Yes	Energy-dependent, $S(E)$	Yes

for some more complex systems.<sup>37</sup> Recently, this was very explicitly demonstrated for the O<sub>2</sub>/Al(111) system,<sup>38</sup> where a first-principles molecular-dynamics study shows the inability of the adiabatic PES to give the correct sticking behavior. For the account of nonadiabaticity with its dissipation to electron-hole pairs, we advocate<sup>39</sup> the use of a diabatic approach.<sup>40</sup>

A few diabatic approaches have been suggested in the literature. One uses a very small number of PES's,<sup>41–43</sup> appropriate for a finite cluster, finds a parametrization that gives an energy dependence of the sticking probability like the measured one, mentions energy dissipation, phonons, and electron-hole pairs, but gives no explicit account thereof. Another one focuses on the PES of the triplet O<sub>2</sub> at the surface, which largely confirms the O<sub>2</sub>/Al curves of Ref. 39 and Fig. 17, and “transitions bringing the system away from the triplet PES,”<sup>44</sup> for whose importance a rough estimate is “provided by the width of the  $2\pi^*$  Kohn-Sham resonance,” which

could be interpreted as the charge-transfer mechanism of Ref. 39, although the energy dissipation issue is not addressed explicitly. We use a diabatic description<sup>39</sup> to account for the nonadiabatic effects and to provide the correct sticking behavior. Here, the continuum of electron-hole-pair states<sup>37,39,45–47</sup> is the obvious channel for the energy dissipation. In Table I, a schematic but systematic overview of the theoretical attempts hitherto to explain the sticking behavior of O<sub>2</sub> on Al(111) is given.

Another aspect of adsorption, the possible existence and properties of a molecularly chemisorbed state, has been addressed in several first-principles studies for diatomic molecules on transition metals. Here a whole range of chemisorption possibilities exist, depending on the adsorbate and the substrate (Table II).

For many of these systems the chemisorption mechanism is explained by the so-called Blyholder model,<sup>48</sup> where the highest occupied molecular orbital (HOMO) and the lowest

TABLE II. Examples of some chemisorption possibilities.

Molecule	Surface	Process	Precursor mediated	Directly activated	Ref.
O <sub>2</sub>	Pt(111)	Dissociation	Low kinetic energies	High kinetic energies	61
O <sub>2</sub>	W(110)	Dissociation	Low kinetic energies	High kinetic energies	62
O <sub>2</sub>	Ir(110)	Dissociation	Low kinetic energies	High kinetic energies	63,64
O <sub>2</sub>	Ge(100)	Dissociation	Low kinetic energies	High kinetic energies	64
O <sub>2</sub>	Ag(111)	Both physi- and chemisorbed molecular states			65
NO	Ni	Molecular and dissociative adsorption			66,67
NO	Ag	Molecular and dissociative adsorption			68,69
NO	Cu	Molecular and dissociative adsorption			70
NO	Pt(111)	Molecularly adsorbed			71
NO	Pd(111)	Molecularly adsorbed			72
CO	Almost all transition metals	Molecularly adsorbed			73
N <sub>2</sub>	Fe(111)	Dissociation	Yes		74
N <sub>2</sub>	W(100)	Dissociation	Yes		75
N <sub>2</sub>	W(110)	Dissociation		Yes	75
N <sub>2</sub>	W(310)	Non-activated dissociation			76

TABLE III. Rough characterization of the molecules with respect to the key parameters electronegativity, Pauli-repulsion range, bond order, and asymmetry for the considered molecules. Trends in sticking and chemisorption are also indicated.

Molecule	F <sub>2</sub>	O <sub>2</sub>	NO	CO	N <sub>2</sub>
Electronegativity	high	medium	medium	low	low
Pauli-repulsion range	short	medium	medium	long	long
Bond order	1	2	2.5	3	3
Asymmetry	none	none	high	high	none
Sticking	high	medium	medium	low	low
Chemisorption bond	strong	medium	medium	weak	weak

unoccupied orbital (LUMO) of the adsorbate are most active in forming the chemisorption bond with *d*-electron states of the underlying transition metal. An electron donation from the adsorbate HOMO to substrate states and a back-donation from such states to the LUMO of the adsorbate build up the chemisorption bond.

Despite a huge number of chemisorption studies of diatomic molecules on transition-metal surfaces, very little attention has been paid to such molecules on simple *sp*-band metals, such as the Al(111) surface. As the latter lack occupied *d*-band states, a study of diatomic molecules on Al(111) should mean a cultivation of chemisorption beyond the Blyholder model.

In this paper, the adsorption of several different diatomic molecules, i.e., F<sub>2</sub>, O<sub>2</sub>, NO, CO, and N<sub>2</sub>, on the Al(111) surface is studied theoretically. There are two foci: (i) to describe the sticking behavior of the considered molecules in a consistent manner, and (ii) to understand the nature of molecular chemisorption. Computer and model studies help us to identify key features: Both issues can be understood in terms of electronegativities, kinetic Pauli-repulsion ranges, bond orders, and asymmetries of the molecules. Electronegativity is defined here as the surface-affected vertical electron affinity. Kinetic Pauli repulsion arises as a result of overlap effects between primarily the HOMO of the molecule and the electronic states of the substrate. Bond order is defined as the number of bonds in the free molecule and provides a measure of the strength of the molecular bond. Asymmetry distinguishes heteronuclear molecules (NO and CO) from homonuclear ones (F<sub>2</sub>, O<sub>2</sub>, and N<sub>2</sub>). The latter property highly affects the character and ordering of the molecular orbitals (MO's) on the energy scale for the considered molecules and thereby also the binding mechanism towards the surface. Table III illustrates the trends in the sticking and chemisorption behaviors for the considered molecules with respect to the key parameters, namely electronegativities, kinetic Pauli-repulsion ranges, bond orders, and asymmetries of the molecules. A detailed explanation of the observed trends is provided throughout the text.

For the sticking behavior, electron transfer from the *sp* bands of the Al(111) surface to the LUMO of the molecule is identified as a key step in the dissociation process. This conclusion comes from extensive DFT calculations on the considered molecules, which provide adiabatic PES's and local densities of states (LDOS). It is observed that electron trans-

fer brings the neutral molecule/Al(111) system to a charged molecule<sup>-δ</sup>/Al(111)<sup>+δ</sup> one ( $\delta$  being the amount of transferred charge), when the molecule is brought closer to the surface. The time scales for the electron transfer process during adsorption and the choice between adiabatic or diabatic descriptions are decisive for the dissociation process. The former description is applicable to situations where the electron transfer process is considerably faster than the motion of the nuclei, causing the LUMO of the molecule to be filled continuously upon approach, or if the charge-transfer process is inactive. The diabatic description is used when the time scales for the electron transfer process and the nuclear motion are comparable, making the details of the charge-transfer process essential. Here it is concluded that a diabatic picture is valuable to account for the observed sticking behaviors of O<sub>2</sub> and NO, while the sticking behaviors of CO, N<sub>2</sub>, and F<sub>2</sub> are fully reconciled in an adiabatic picture. In addition, the electron-transfer process provides a necessary dissipation channel into the sea of substrate electron-hole pairs, to which a coupling is introduced into the system during the adsorption process. Hence, kinetic and dissociation energies of the adsorbate are lost into electronic degrees of freedom, all in agreement with experimental evidence.<sup>21,22</sup>

Furthermore, among the considered molecules, F<sub>2</sub> and N<sub>2</sub> are the only ones that are not adsorbed molecularly on the surface. O<sub>2</sub> and NO exhibit molecularly chemisorbed states, identified as having "O<sub>2</sub><sup>2-</sup>" and "NO<sup>2-</sup>" electron configurations, respectively. The CO molecule has a neutral molecular state for an orientation parallel to the surface and a charged one, identified as a "CO<sup>-</sup>" configuration, for the perpendicular orientation with the C atom facing the surface. To understand the nature of the molecularly chemisorbed states, bond order and asymmetry really matter. The bond order basically tells how many electrons can be transferred to the molecule before it dissociates. However, this number can be reduced, when the adiabatic PES's indicate the existence or favorable energy of a molecularly chemisorbed state.

The plan of the paper is as follows. Section II gives extensive accounts of the adiabatic calculations. The results include PES's and LDOS's. In Sec. III, the diabatic picture is presented, with foci on the calculation of diabatic PES's and on the sticking model. Discussions of a consistent theory for the sticking behaviors of diatomic molecules on an *sp*-band metal, such as Al(111), and on the existence of molecularly chemisorbed states are given in Sec. IV. The paper ends with conclusions and an outlook for future work.

TABLE IV. Molecular properties for all of the considered molecules in this study, as described by DFT. In parentheses are the experimental values.

Molecule	Bond distance (Å)	Vibrational frequency (cm <sup>-1</sup> )	Dissociation energy (eV)
F <sub>2</sub>	1.43 (1.41)	1040 (916)	3.4 (1.6)
O <sub>2</sub>	1.24 (1.21)	1620 (1580)	5.6 (5.1)
NO	1.18 (1.16)	1960 (1904)	6.7 (5.1)
CO	1.16 (1.13)	2230 (2170)	12.4 (11.1)
N <sub>2</sub>	1.12 (1.09)	2430 (2358)	9.6 (9.8)

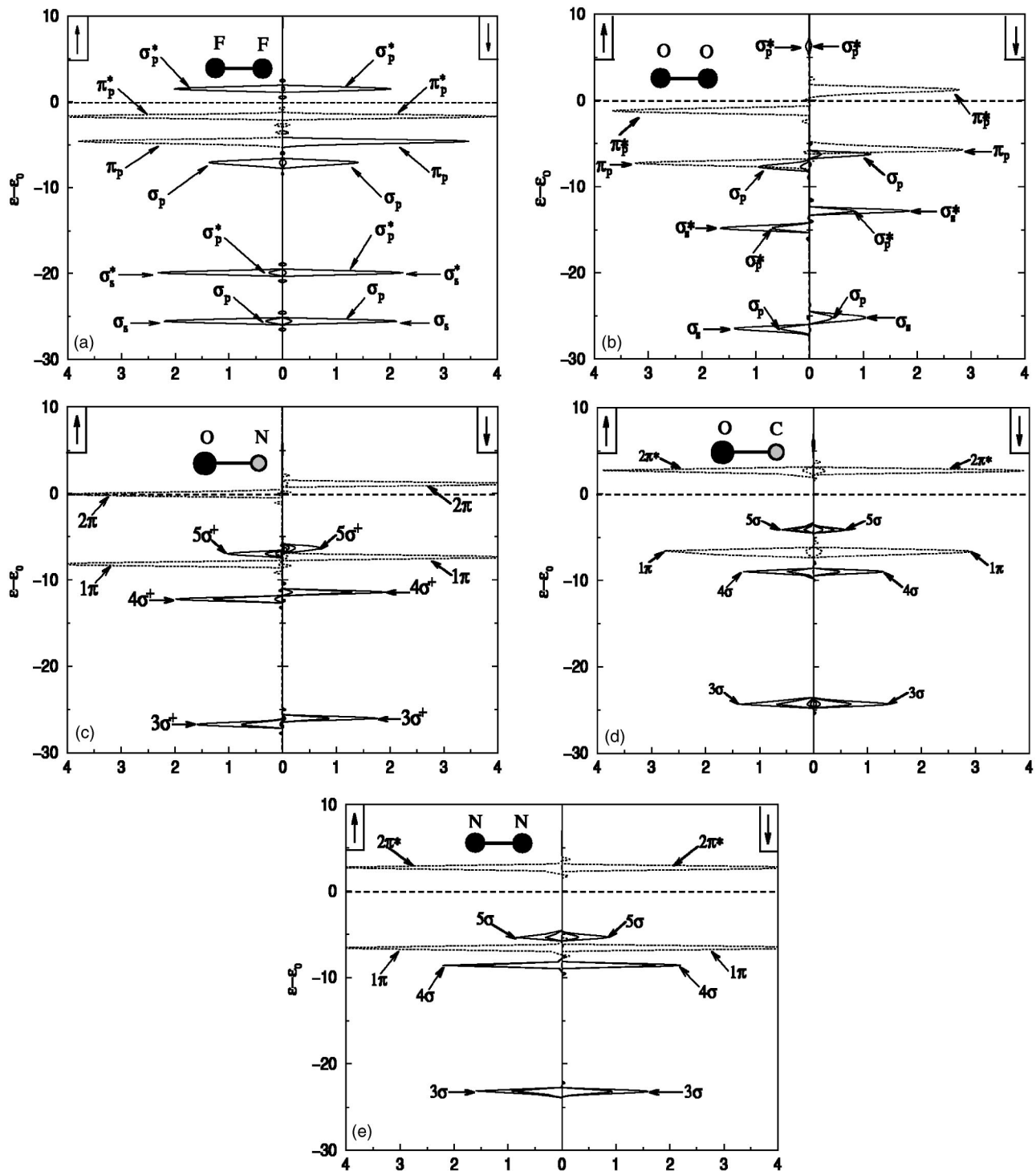


FIG. 1. Energy levels of the molecular orbitals (MO) of the free (a)  $F_2$ , (b)  $O_2$ , (c)  $NO$ , (d)  $CO$ , and (e)  $N_2$  molecules, calculated within the present method. The local densities of states (LDOS's) are projected into MO's. The left and right panels show the spin-up and -down LDOS's, respectively.

## II. ADIABATIC PICTURE

The ground-state adiabatic calculations performed with DFT (Ref. 27) concern total energies and various aspect of the electron structure, such as densities and local densities of Kohn-Sham energy levels (LDOS), i.e., entities that are important for both adiabatic and diabatic descriptions.

The calculations presented in this paper are performed by means of the plane wave pseudopotential code DACAPO.<sup>49</sup> The generalized-gradient approximation<sup>50-52</sup> (GGA) is used for the exchange-correlation energy-density functional, more specifically the PW91 flavor. The wave functions are expanded in a plane-wave basis set with an energy cutoff of

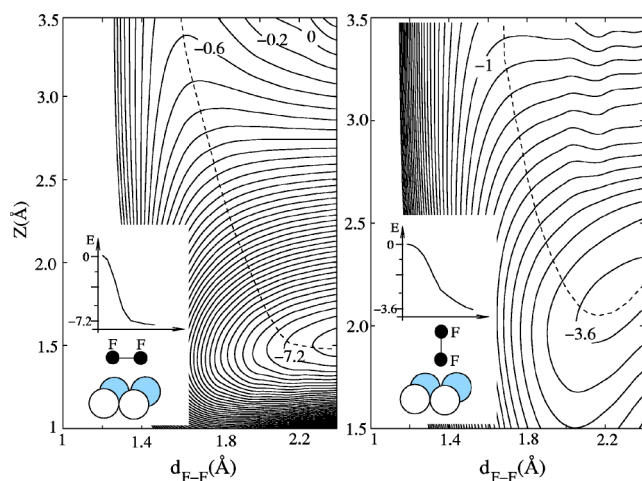


FIG. 2. Cuts through the six-dimensional potential-energy surface (PES) of  $F_2$  with bond length  $d_{F-F}$ , a distance  $Z$  above the Al(111) surface layer; parallel above the fcc site (left) and perpendicular above fcc site (right). In the inset, the 1D PES along the reaction path (dashed line) are shown.

25 Ry, and the electron-ion interactions are described by ultrasoft pseudopotentials. A  $8 \times 8 \times 1$  Monkhorst-Pack mesh is used to sample the entire Brillouin zone. Any induced dipole moment is compensated for by an effective dipole correction.<sup>53</sup> The system consists of six layers of Al and five vacuum layers in a  $2 \times 2$  supercell. The local density of states (LDOS) is obtained by projection on the orbitals of the local unit under consideration, including an effective broadening of 0.2 eV.

### A. Free molecules

As GGA functionals, such as the PW91, describe some free molecule rather poorly, we give bond distances, vibrational frequencies, and dissociation energies for all the considered molecules, see Table IV. The overall agreement is reasonable considering the problems associated with DFT and free molecules.

Electron transfer from surface to adsorbate is a key to dissociation.<sup>26,27,39</sup> This sets the focus on adsorption effects on molecular orbitals (MO's), here as LDOS's projected onto MO's (Fig. 1). The studied molecules have the obvious similarity of having bonding and antibonding orbitals of both  $\pi$  and  $\sigma$  types present. There are basically three major differences.

(i) The ordering of the MO's with respect to energy. For  $O_2$  and  $F_2$ , the bonding  $\sigma$  MO's are lower in energy than the bonding  $\pi$  MO's, for both spins. For  $N_2$ , NO, and CO, on the other hand, this ordering is reversed. The order has important consequences for the orientational dependence of the initial sticking and for the molecular bond to the surface.

(ii) Spin splittings are sizable (2 eV) for both bonding and antibonding MO's, of  $\pi$  as well as  $\sigma$  type, for both  $O_2$  and NO. This reflects Hund's spin rule, which describes ground states as spin-compensated ( $S=0$  for CO,  $N_2$ , and  $F_2$ ) and -polarized ( $S=1$  for  $O_2$  and  $S=1/2$  for NO), respectively.

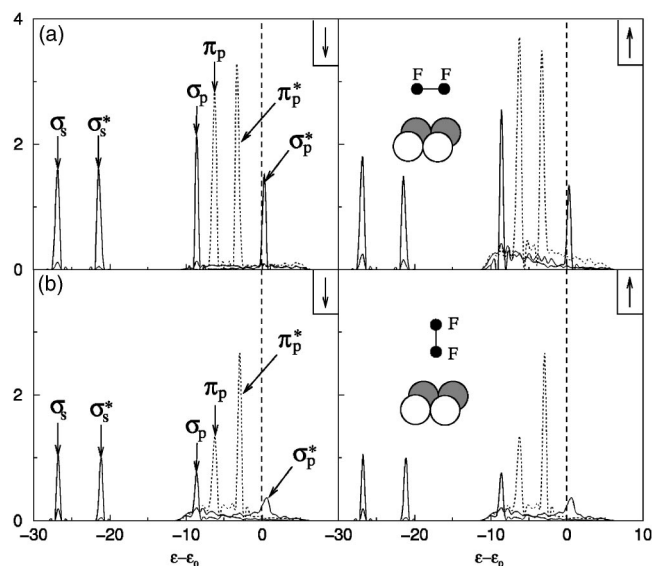


FIG. 3. The LDOS for the  $F_2$  molecule above the fcc site with (a)  $(Z, d_{F-F}, \theta) = (3.0, 1.45, 90^\circ)$ , and (b)  $(Z, d_{F-F}, \theta) = (3.0, 1.45, 0^\circ)$ . The left and right panels show the spin-up and -down LDOS's, respectively. The dashed line is the Fermi level.

(iii) The bond orders and electronegativities vary considerably, CO and  $N_2$  (NO and  $O_2$ ;  $F_2$ ) having bond orders of 3 (2; 1) and low (intermediate; high) electronegativities, respectively. This has implications on both sticking and molecular adsorption.

## B. Admolecules

The calculated adiabatic PES for diatomic molecules at the Al(111) surface are presented as PES cuts, which are functions of the molecular center of mass (CM) distance to the surface-Al layer,  $Z$ , and the separation between the atoms,  $d$ . The CM is placed above the high-symmetry fcc site, the energetically most favorable site for  $O_2$  and NO far outside the surface ( $Z \leq 4$  Å). The results for each molecule are shown with two different orientations of the molecule, with its axis parallel and perpendicular to the surface, respectively. For the heteronuclear molecules NO and CO, both the oxygen atom down (O end-on) and up (N and C end-on, respectively) orientations are represented.

### 1. $F_2$ molecule

For the  $F_2$  molecule (Fig. 2) the energy goes downhill as the molecule approaches the surface for all orientations, implying the absence of any activation-energy barrier in the entrance channel. As a result, the sticking probability is unity, independent of the initial translational energy of the incoming  $F_2$  molecules. This result is in agreement with experimental findings.<sup>22</sup>

The calculated LDOS's for the  $F_2$  molecule (Fig. 3) in the parallel [ $(Z, d_{F-F}, \theta) = (3.0, 1.45, 90^\circ)$ ] and perpendicular orientations [ $(Z, d_{F-F}, \theta) = (3.0, 1.45, 0^\circ)$ ] clearly illustrate that there are interference effects between the MO's of  $F_2$  and the electronic states of the Al(111) surface. This effect is more

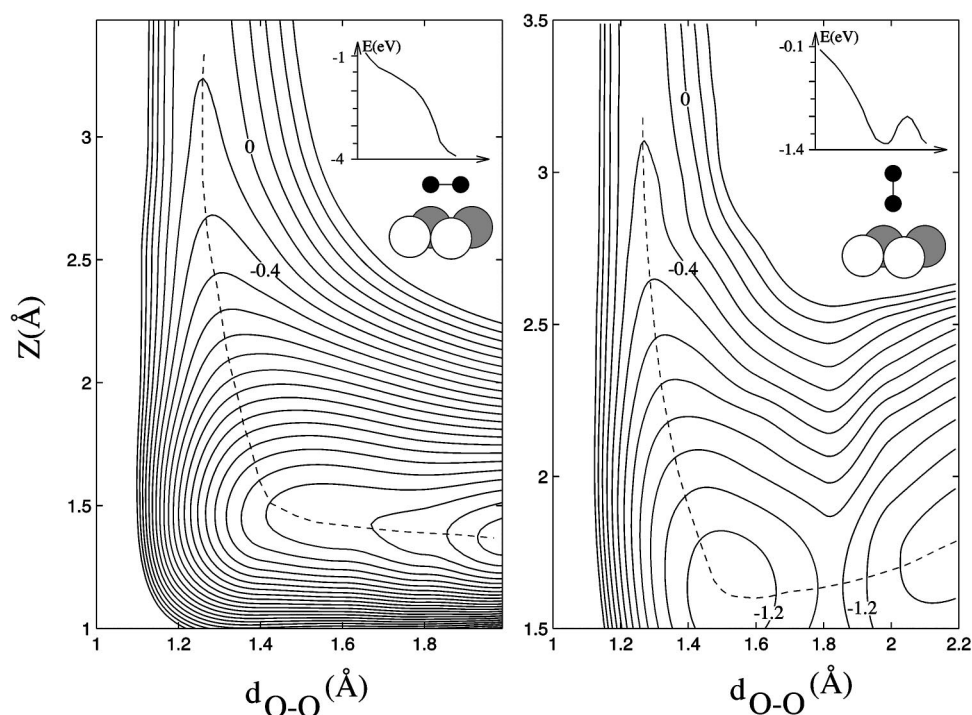


FIG. 4. Cuts through the six-dimensional PES of O<sub>2</sub> as a function of bond length  $d_{\text{O-O}}$  and distance  $Z$  above the Al(111) surface parallel (left) and perpendicular (right) to the surface above an fcc site. In the inset, the 1D PES along the reaction path (dashed line) are shown.

evident for the perpendicular orientation, demonstrating the stronger overlap of the inner-F-atom orbitals with the surface states at a given  $Z$ .

For both orientations, it can be concluded that the forces from the attractive “F<sub>2</sub><sup>-</sup>/Al<sup>+</sup>(111)” and “F<sub>2</sub><sup>2-</sup>/Al<sup>2+</sup>(111)” PES’s act far outside the surface. At the same time, the repulsive neutral “F<sub>2</sub>/Al(111)” forces act much further in. This implies that electron transfer from the surface to the LUMO of F<sub>2</sub> is active far out.

Another observation is that the perpendicular orientation is energetically favored early in the entrance channel. The antibonding  $\sigma^*$  LUMO of the F<sub>2</sub> molecule, empty in the free molecule but filled upon molecular approach to the surface, overlaps with the Al states further out in this orientation. When the first electron transfer to it has occurred, the F<sub>2</sub> molecule can rotate to the parallel orientation, which is energetically favored closer to the surface.

In the PES for the perpendicular orientation, the possibility of emission of one of the F atoms is indicated. Here, the bond length  $d_{\text{F-F}}$  of a molecule grows with the CM coordinate  $Z$  downhill along the minimum-energy path, ultimately beyond our computational limits. This abstraction channel is exothermic according to our calculations by about 2.6 eV, the dissociation energy of the free F<sub>2</sub> molecule being 2.25 eV and the chemisorption energy of the F atom on the surface being 4.81 eV.

For the F<sub>2</sub>/Al(111) system, the calculated PES lacks a molecularly adsorbed state. The rationale for this is the high electron affinity of the F atom, which thermodynamically favors dissociation. Further, the fact that F<sub>2</sub> has a bond order of unity favors the dynamics, the first electron transfer to the antibonding  $\sigma^*$  MO placing most of the energy into the internal vibrational coordinate, which initiates the bond breaking and makes the second electron transfer inevitable, leading to the dissociation.<sup>46</sup>

## 2. O<sub>2</sub> molecule

Our calculated adiabatic PES cuts for the O<sub>2</sub>/Al(111) (Refs. 26 and 27) lack energy barriers in the entrance channel, both for the parallel and perpendicular orientations, similar to the F<sub>2</sub>/Al(111) system (Fig. 4). The traditional sticking description<sup>25</sup> then implies a nonactivated dissociation process. If the O<sub>2</sub> molecules would follow the adiabatic PES, they should stick to the surface with 100% probability, independent of their initial translational energy. This is in contradiction to experimental findings.<sup>21</sup>

Another essential issue in understanding the sticking is the electron-transfer process, which initiates the sticking process.<sup>39</sup> The presence of electron transfer can be observed in the calculated LDOS’s (Fig. 5) for the parallel  $[(Z, d_{\text{O-O}}, \theta) = (3.0, 1.24, 90^\circ)]$  and perpendicular  $[(Z, d_{\text{O-O}}, \theta) = (3.0, 1.24, 0^\circ)]$  orientations. Already at  $Z = 3 \text{ \AA}$ , the  $2p_{x,y}$ -derived minority-spin  $\pi^*$  resonance, which is empty in the free oxygen molecule, is shifted slightly in energy and becomes partially occupied. This shows that under adiabatic conditions, i.e., when electrons have been given infinite time to adjust, electronic charge is transferred from the surface to the molecule. Due to the antibonding character of the  $\pi^*$  orbital, the intramolecular bond then weakens, and the dissociation process starts.<sup>46,47</sup> Under the dynamical conditions associated with sticking, there is a competition between the electron tunneling process and the motion of the nuclei that causes the occupancy of the  $\pi$  resonance to depend on the initial translational energy of the adsorbate.

The trends in the energetics of the O<sub>2</sub>/Al(111) system are similar to those of F<sub>2</sub>/Al(111) but less pronounced. The steering effect has important effects on the orientation of an incoming thermal O<sub>2</sub> molecule. According to the adiabatic PES and the Hellman-Feynman forces derived from it, a change in orientation of the O<sub>2</sub> molecules from perpendicular

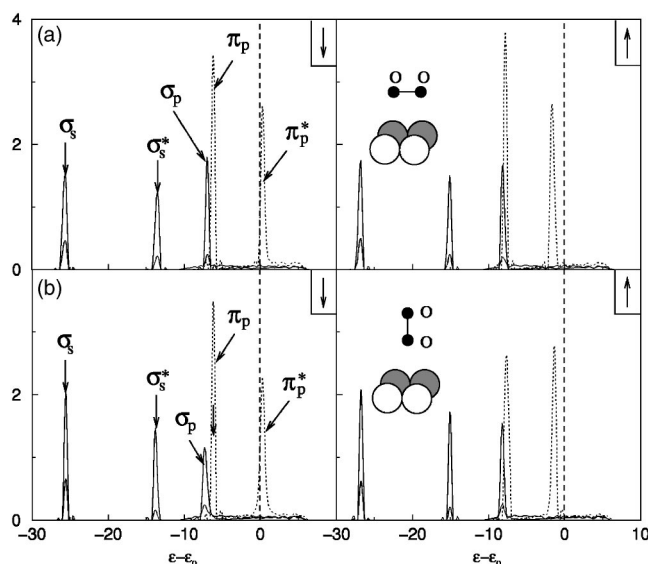


FIG. 5. The local density of states (LDOS) for the  $O_2$  molecule above the fcc site with (a)  $(Z, d_{O-O}, \theta) = (3.0, 1.24, 90^\circ)$  and (b)  $(Z, d_{O-O}, \theta) = (3.0, 1.24, 0^\circ)$ . The left and right panels show the spin-up and -down LDOS's, respectively. The dashed line is the Fermi level.

to parallel is found to be hindered by an energy barrier, even relatively far out from the surface. Furthermore, the van der Waals energy favors the perpendicular orientation, by about 7 meV at  $Z = 3.5 \text{ \AA}$ .<sup>26,27</sup> Molecules approaching the surface in the perpendicular orientation are apt for abstraction, something that has been observed experimentally for  $O_2/\text{Al}(111)$ .<sup>24</sup>

The molecularly chemisorbed state, which has a calculated well depth of 0.25 eV,<sup>27</sup> should have great consequences for the continued dynamics of the oxygen molecules on the surface.<sup>54</sup> From calculated LDOS's, it is concluded that this metastable molecular state has an " $O_2^{2-}$ " electronic configuration and is stabilized by the very nonequivalent Al-surface forces on the oxygen atoms of the nonparallel  $O_2$  molecule.<sup>26,27</sup> Recent experiment set an upper limit to the depth of any molecularly chemisorbed state to 0.1 eV.<sup>55</sup> Our too high value is within the expected accuracy depending on the flavor of the exchange-correlation functional. However, here we utilize the option provided by theory to study trends among the molecular chemisorbed states on the Al(111) surface.

### 3. NO molecule

For the NO molecule, both the atomic asymmetry and the unpaired electron in the antibonding  $2\pi^*$  orbital have substantial effects on the PES and make the NO/Al(111) system quite different from the  $F_2/\text{Al}(111)$  and  $O_2/\text{Al}(111)$  systems. However, there are some similarities, such as the absence of an absolute energy barrier in the entrance channel, the active role of charge transfer in the dissociation process, and the existence of a molecularly chemisorbed state.

For both parallel and N end-on orientations, the calculated adiabatic PES cuts for the NO/Al(111) system (Figs. 6 and

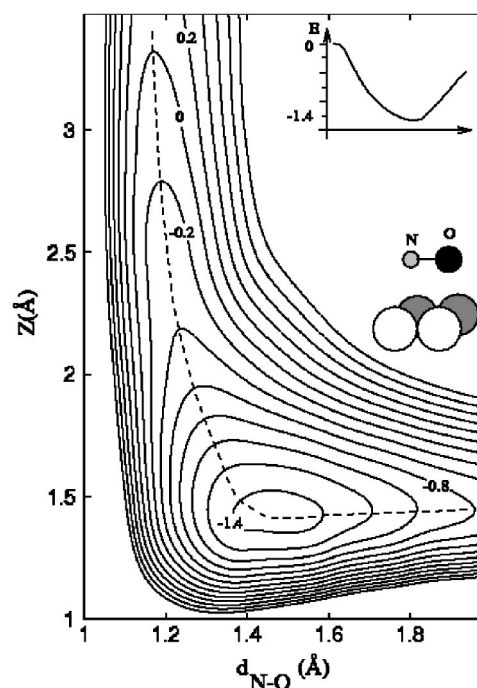


FIG. 6. Cuts through the six-dimensional PES of NO as a function of bond length  $d_{N-O}$  and distance  $Z$  of the CM from the Al(111) surface layer, above the fcc site, and with the molecular axis parallel to the surface (the side-on orientation). The numbers in the equipotential contours are the energy values in eV measured from the energy of the totally separated NO and Al surface. The inset gives the energy of the system along the reaction path (indicated by a dashed line).

7) are similar to the  $F_2/\text{Al}(111)$  and  $O_2/\text{Al}(111)$  systems, being attractive for both parallel and the N end-on orientations and lacking energy barriers in the entrance channel. For the O end-on orientation, on the other hand, the PES is repulsive in the entrance channel, with an energy barrier of 0.6 eV into the dissociation channel. This energy barrier alone cannot make the dissociation activated. Judging from the calculated Hellmann-Feynman forces acting far outside the surface, low-speed NO molecules should be aligned in the N end-on orientation. As for the  $O_2/\text{Al}(111)$  system, the experimentally observed sticking behavior<sup>22</sup> is not reconciled with our adiabatic calculation and calls for a nonadiabatic one, discussed in the next section.

Among the considered orientations, the N end-on one is energetically favored, thanks to effective charge transfer for this orientation. This is seen in the calculated LDOS's at  $Z = 3.0 \text{ \AA}$  (see Fig. 8), where the downshift of antibonding  $2\pi^*$  MO energy is largest for the N end-on orientation, while the surface effects are almost absent for the two other orientations.

The physical reasons behind the activation-energy barrier in the O end-on orientation are indicated by the LDOS's calculated at some relevant points  $[(Z, d_{N-O}) = (3.0, 1.2), (2.5, 1.25), \text{ and } (2.0, 1.4 \text{ \AA})]$  along the minimum energy path (Fig. 9). Compared to the free NO molecule, the antibonding  $2\pi^*$  resonance has only a small shift down in energy and is filled with about one additional electron, while the  $2\sigma$  resonance

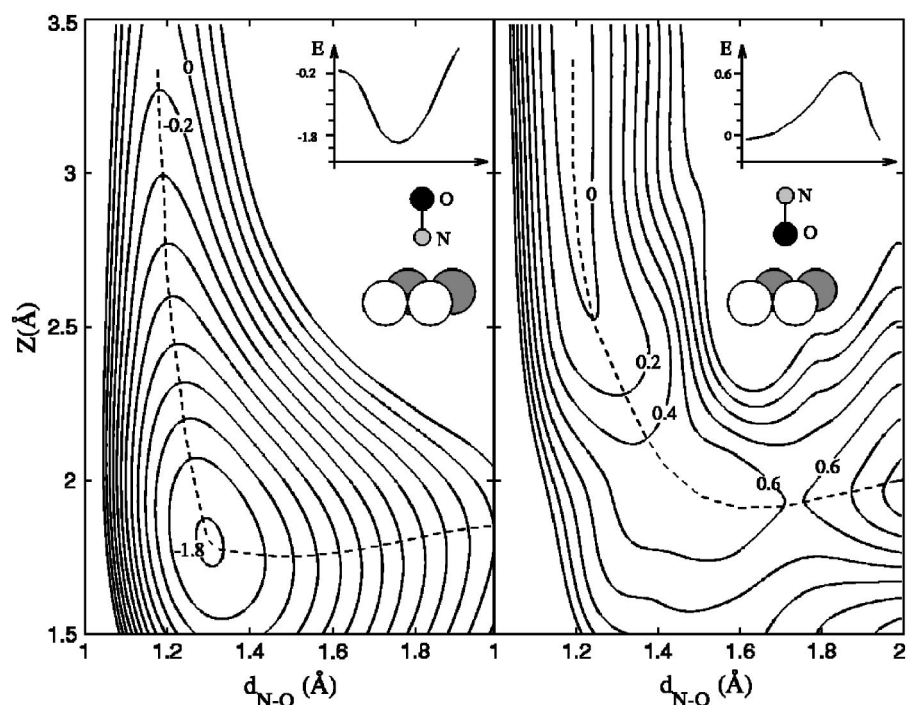


FIG. 7. Cuts through the six-dimensional PES of NO as a function of bond length  $d_{\text{N-O}}$  and distance  $Z$  above the Al(111) surface layer, above the fcc site with the molecular axis perpendicular to the surface (the head-on orientation). The left and right panels show the PES's for the N end-on and O end-on orientations, respectively. The numbers in the equipotential contours are the energy values in eV measured from the energy of totally separated NO on Al surface.

maintains its energy, even at  $Z=2.0$  Å. In comparison, the N end-on orientation (Fig. 8) shows some interference between NO MO's and Al electron states already at  $Z=3.0$  Å. Hence, for the orientation with O end-on, compared to N end-on, the attractive “NO<sup>-</sup>/Al(111)<sup>+</sup>” or “NO<sup>2-</sup>/Al(111)<sup>2+</sup>” PES's lie much further in and the repulsive “NO/Al(111)” PES's much further out compared to the N end-on configuration.

For parallel and N end-on orientations, NO is calculated to have a molecularly chemisorbed state. Calculated LDOS's

(Fig. 10) for side-on  $[(Z, d_{\text{N-O}})=(1.5, 1.4)$  Å] and end-on  $[(Z, d_{\text{N-O}})=(1.8, 1.3)$  Å] NO show the antibonding spin-up and -down  $2\pi^*$  energy levels to be downshifted to energies below the Fermi level and filled up with two extra electrons, resulting in an “NO<sup>2-</sup>” electron configuration of that molecular state. Energy shifts also apply to the  $4\sigma$  and  $5\sigma$  MO's, which couple strongly to the Al conduction electrons, but with no change in occupancy.

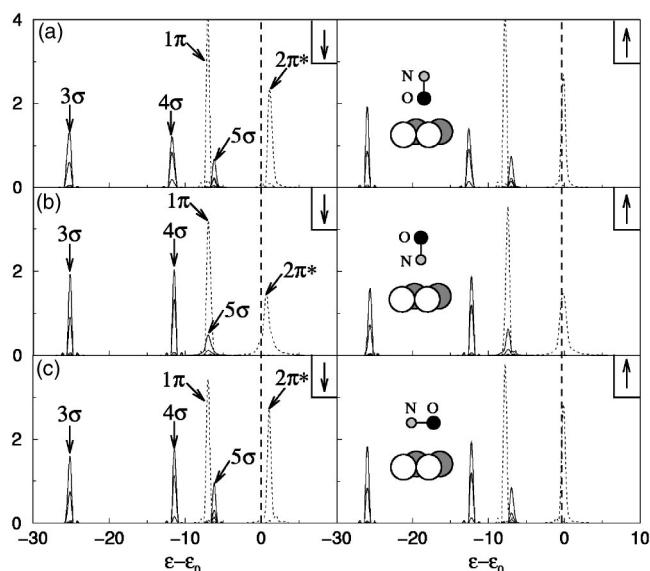


FIG. 8. The local density of states (LDOS) for the NO molecule above the fcc site with (a)  $(Z, d_{\text{N-O}}, \theta)=(3.0, 1.2$  Å,  $0^\circ$ ) with O facing the surface, (b)  $(Z, d_{\text{N-O}}, \theta)=(3.0, 1.2$  Å,  $0^\circ$ ) with N facing the surface, and (c)  $(Z, d_{\text{N-O}}, \theta)=(3.0, 1.2$  Å,  $90^\circ$ ). The left and right panels show the spin-up and -down LDOS's, respectively. The dashed line is the Fermi level.

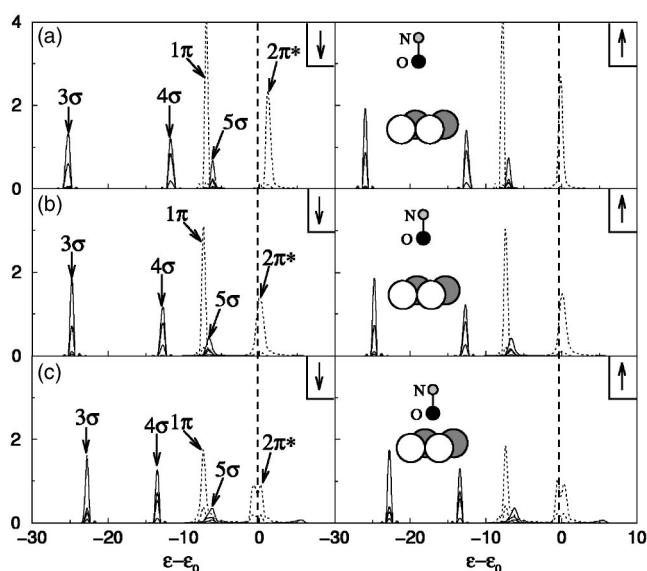


FIG. 9. Local density of states (LDOS) for the NO molecule perpendicular to the surface, with oxygen down, above the fcc site with (a)  $(Z, d_{\text{N-O}}, \theta)=(3.0, 1.2$  Å,  $0^\circ$ ), (b)  $(Z, d_{\text{N-O}}, \theta)=(2.5, 1.25$  Å,  $0^\circ$ ), and (c)  $(Z, d_{\text{N-O}}, \theta)=(2.0, 1.4$  Å,  $0^\circ$ ). The left and right panels show the spin-up and -down LDOS's, respectively. The dashed line is the Fermi level.



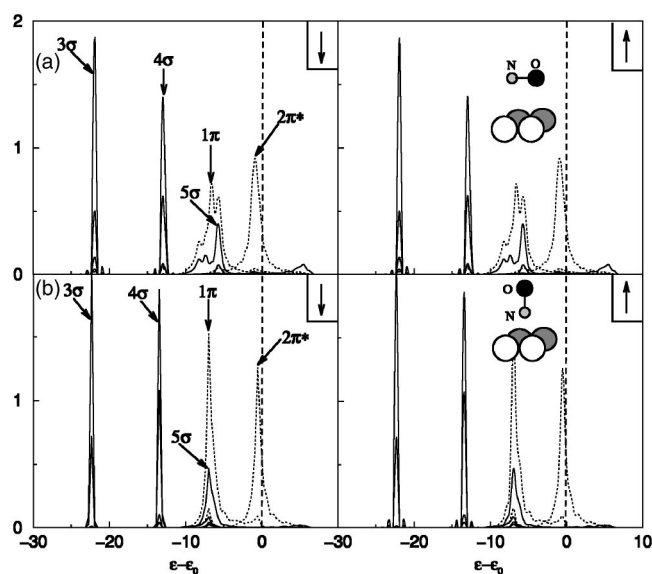


FIG. 10. The local density of states (LDOS) for the NO molecule above the fcc site with (a)  $(Z, d_{N-O}, \theta) = (1.5, 1.4 \text{ \AA}, 90^\circ)$  and (b)  $(Z, d_{N-O}, \theta) = (1.3, 1.8 \text{ \AA}, 0^\circ)$  with N facing the surface. The left and right panels show the spin-up and -down LDOS's, respectively. The dashed line is the Fermi level.

The bond order is higher in NO than in  $O_2$ , which means that more electrons, in principle, can be transferred to the NO before it dissociates. In addition, the access to a large number of transferred electrons make NO bind more strongly to the surface. The energetics, Fig. 8, show that only two electrons have been transferred to get the adiabatic “NO<sup>2-</sup>” ground state, thus the intermolecular bond in NO is still strong. However, as for  $O_2$ , dissociation is the likely easy-decay channel, although Figs. 6 and 7 show this to occur along a slightly different route.<sup>31</sup>

#### 4. CO molecule

The free CO molecule differs from the above ones, having all its bonding  $\pi$  and  $\sigma$  MO's occupied and the corresponding antibonding ones empty, a large HOMO-LUMO gap, and a spin-compensated ground state ( $S=0$ ). Furthermore, in the CO/Al(111) interaction, charge transfer is not efficient enough to reduce the bond order. As a consequence, the adiabatic picture should be adequate to account for the observed sticking behavior in this case.<sup>22</sup>

The adiabatic PES cuts calculated for the CO molecule (Figs. 11 and 12) show an energy barrier in the entrance channel for all considered orientations, with heights 0.3 and 0.1 eV for the parallel and C end-on orientations, respectively, while the O end-on orientation is repulsive for all CM distances. The calculated LDOS's for side-on, C end-on, and O end-on orientations at  $Z=3.0 \text{ \AA}$  (Fig. 13) show the electronic structure of the CO molecule to be almost identical to that of the free molecule.

As in the NO/Al(111) system, the atomic asymmetry of CO causes the antibonding  $\sigma$  and  $\pi$  orbitals to be shifted towards the C atom, which in turn gives charge transfer only for the C end-on orientation. Atomic asymmetry is also im-

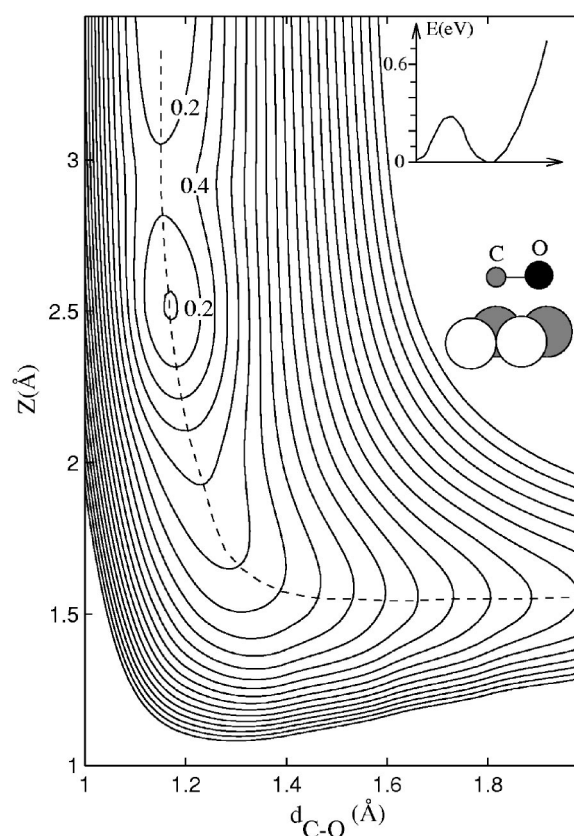


FIG. 11. Cuts through the six-dimensional PES of CO as a function of bond length  $d_{C-O}$  and distance  $Z$  of the CM from the Al(111) surface layer, above the fcc site, with the molecular axis parallel to the surface (the side-on orientation). The numbers in the equipotential contours are the energy values in eV measured from the energy of totally separated CO and Al surface. The inset gives the energy of the system along the reaction path (indicated by a dashed line).

portant for the existence of molecularly adsorbed states, as shown by the adiabatic PES (Figs. 11 and 12). CO parallel to the surface has a shallow molecular state (depth: 0.1 eV). For the C end-on orientation, the PES is similar, however, with a molecular state position closer to the surface and a 0.4 eV deeper well. The calculated LDOS's (Fig. 14) at  $[(Z, d_{C-O}, \theta) = (2.5, 1.2 \text{ \AA}, 90^\circ)]$  and C end-on  $[(Z, d_{C-O}, \theta) = (2.0, 1.2 \text{ \AA}, 0^\circ)]$  distinguish between the molecularly adsorbed states in the parallel and end-on orientations: The former have just antibonding  $\pi$  levels (both spin up and down) downshifted slightly, otherwise being almost identical to that of the free molecule. In effect, this blocks electron transfer to the antibonding resonances, and the latter ones have (i) a much larger downshift of the antibonding  $\pi$  levels, the LDOS showing a transfer of one electron to the antibonding  $\pi$  resonance, making this state a “CO<sup>-</sup>” state, and (ii) a bonding  $5\sigma$  resonance that is downshifted considerably and that couples strongly to the Al surface electrons.

#### 5. N<sub>2</sub> molecule

The N<sub>2</sub> molecule also has a bond order of 3 and is electronically like CO but symmetric. The calculated adiabatic PES cuts (Fig. 15) are repulsive for all CM distances and

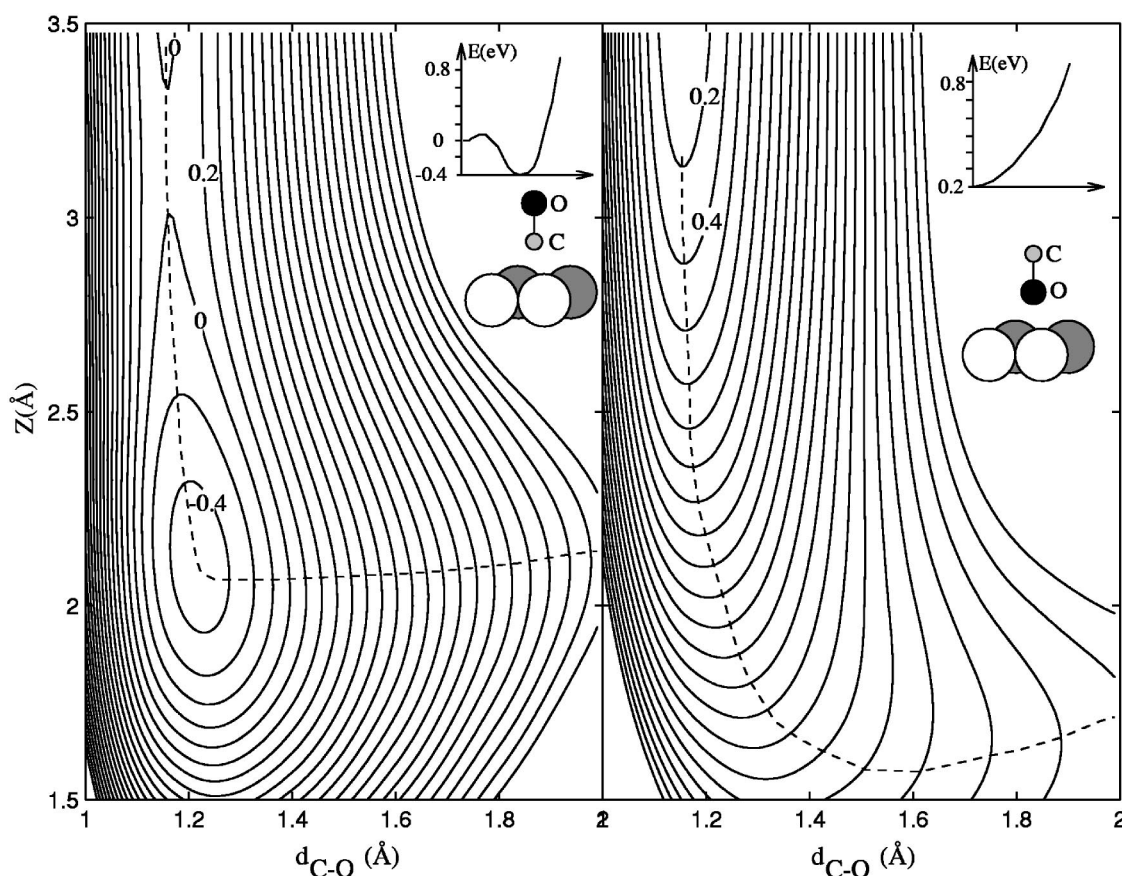


FIG. 12. Cuts through the six-dimensional PES of CO as a function of bond length  $d_{\text{C-O}}$  and distance  $Z$  above the Al(111) surface layer, above the fcc site, with the molecular axis perpendicular to the surface (the head-on orientation). The left and right panels show the PES's for CO with the C and O atom facing the surface, respectively. The numbers in the equipotential contours are the energy values in eV measured from the energy of the totally separated CO and Al surface.

orientations. Compared to CO, differences in MO overlaps with the surface electronic states make the kinetic-energy repulsion more effective early in the entrance channel for all orientations, at a given  $Z$  value. The calculated LDOS's (Fig. 16) at  $Z=3.0$  Å show the electronic structure of  $\text{N}_2$  here to be identical to that of the free molecule, independent of orientation. Thus the image-modified LUMO crosses the Fermi level very close to the surface. With the " $\text{N}_2^-/\text{Al}(111)^+$ " and " $\text{N}_2^{2-}/\text{Al}(111)^{2+}$ " PES's close to the surface and the neutral  $\text{N}_2/\text{Al}(111)$  PES repulsive far out, the approaching  $\text{N}_2$  molecule keeps its bonding MO's filled and its antibonding MO's empty, and it upholds its wide HOMO-LUMO gap and its strong intramolecular bond, making charge transfer inactive in the molecule-surface reaction and thus staying inert. This result is in good agreement with experimental findings,<sup>22</sup> which show that the adiabatic PES's are sufficient to account for the sticking behavior. Because of this low surface electronegativity, the  $\text{N}_2/\text{Al}(111)$  system also lacks a molecularly adsorbed state. Its high bond order expresses the fact that a large number of electrons have to be transferred to the MO's before  $\text{N}_2$  dissociates.

As a side comment, the effect of an additional molecule-surface attraction can be mentioned. A hypothetical extra overlap between the  $\text{N}_2$  LUMO and some substrate electron states could downshift the LUMO resonance further and

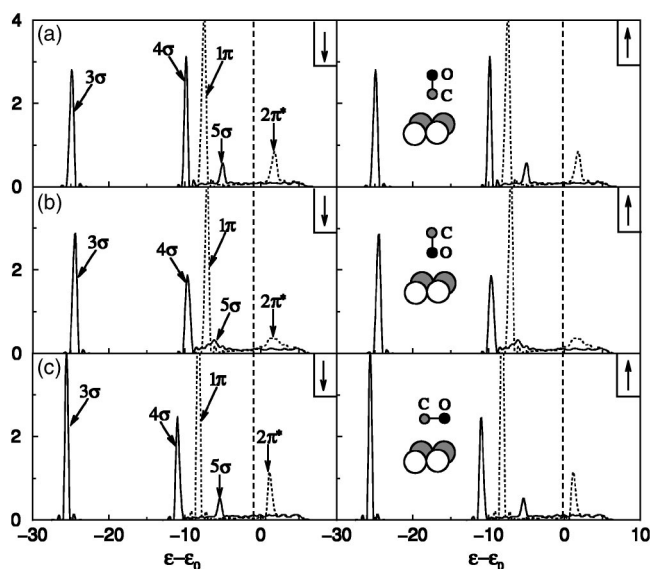


FIG. 13. The local density of states (LDOS) for the CO molecule above the fcc site with (a)  $(Z, d_{\text{C-O}}, \theta) = (3.0, 1.16 \text{ Å}, 0^\circ)$  with O facing the surface, (b)  $(Z, d_{\text{C-O}}, \theta) = (3.0, 1.16 \text{ Å}, 0^\circ)$ , with C facing the surface, and (c)  $(Z, d_{\text{C-O}}, \theta) = (3.0, 1.16 \text{ Å}, 90^\circ)$ . The left and right panels show the spin-up and -down LDOS's, respectively. The dashed line is the Fermi level.

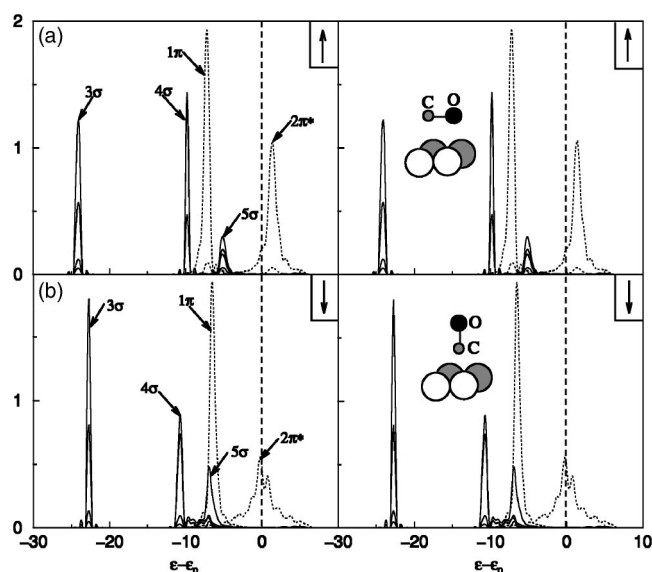


FIG. 14. The local density of states (LDOS) for the CO molecule above the fcc site with (a)  $(Z, d_{C-O}, \theta) = (2.0, 1.2 \text{ \AA}, 90^\circ)$  and (b)  $(Z, d_{C-O}, \theta) = (2.5, 1.2 \text{ \AA}, 0^\circ)$  with C facing the surface. The left and right panels show the spin-up and -down LDOS's, respectively. The dashed line is the Fermi level.

make the image- and interference-modified LUMO cross the Fermi level further out from the surface, maybe in the region early in the entrance channel with its effective kinetic-energy repulsion. Such a situation is present on transition-metal surfaces, where in some cases the  $d$  electrons can have marginal effects important for sticking, molecular adsorption, and catalysis.

A similar marginal effect is noticed in the comparison with the isoelectronic CO molecule. Actually, the lack of asymmetry in  $N_2$  reduces its overlap with the surface, even with the free-electron-like Al surface. The asymmetry of the CO makes the  $5\sigma$  MO both reside primarily on the carbon atom and possess an energy level in the range of the Al  $s$ -electron states, which are the conduction electrons providing the right symmetry for a nonzero overlap with the  $5\sigma$  MO. This small  $5\sigma$  "donation" and the tiny  $2\pi^*$  "back donation" make the CO bond to the Al surface stronger than that of  $N_2$ , whose symmetry is unfavorable for orbital overlap and energy match.

### III. STICKING AND DIABATIC PICTURE

As discussed earlier, electron transfer from surface states to the LUMO of the molecule is the key process that initiates the dissociation event. For NO and  $O_2$  with lower electronegativities than for  $F_2$  and larger than for CO and  $N_2$ , the time for the electron transfer process is comparable to that of the nuclear motion in the "reaction zone." In turn, this gives rise to nonadiabatic processes and electron transfer events.<sup>37</sup> Actually, transport of charge should be part of a full account for the observed sticking behavior for these molecules, and a diabatic description is adequate.<sup>39,46</sup> For  $F_2$ ,  $N_2$ , and CO, on the other hand, the adiabatic and diabatic descriptions yield the same result (see below).

In order to understand the sticking behavior in a diabatic picture, the following key steps are considered: (i) Diabatic PES's for the relevant systems are calculated, for instance, by use of our recently proposed method for excited states.<sup>56</sup> The latter is a DFT-based method, which can be viewed as a generalization of the  $\Delta$ SCF method.<sup>57</sup> (ii) The sticking behavior is modeled by means of a simple one-dimensional charge-transfer model.<sup>39</sup> The present model differs from that of Ref. 39 by the care in calculating the PES's.

#### A. Potential-energy surfaces

In our method for calculating electronically excited PES's within the DFT framework,<sup>56</sup> an electronically excited state is calculated using a Kohn-Sham (KS) determinant constructed by other KS orbitals than the  $N$  lowest ones, in order to accommodate  $e$ - $h$  pair excitations. The KS orbitals of the  $e$ - $h$  pair excitations are chosen based on the information provided by the LDOS's from the ground-state DFT calculation, together with the assumption that charge transfer to the LUMO of the adsorbate is the key mechanism for sticking on simple  $sp$ -band metals. Thus, the electronically excited states can be described as the neutral  $X_2/Al(111)$  state and the charged-transferred ones as the  $X_2^-/Al^+(111)$  state, etc. ( $X_2$  being the considered molecule). The calculation of these excited states involves the following steps.

(i) A standard ground-state DFT calculation is performed, using the supercell method. This yields the KS orbitals for the ground-state  $X_2^\delta/Al(111)^{+\delta}$  system ( $\delta$  being the transferred charge) and their corresponding discrete eigenenergies for each  $k$  point. Eigenenergies for each considered KS orbital are identified with the help of LDOS's calculated for several molecule-surface separations.

(ii) The electronically excited configurations, namely the  $X_2/Al(111)$  and  $X_2^-/Al^+(111)$  states, are constructed by introducing  $e$ - $h$  pairs into the electronic system, i.e., using a Slater determinant with  $N-1$  of the above-mentioned KS orbitals ( $h$ ) and one other KS orbital ( $e$ ) occupied [knowledge of the MO structure for the free  $X_2$  molecule (Fig. 1) is instructive here]. Such an  $e$ - $h$  pair signifies an internal charge transfer between initially occupied and unoccupied KS orbitals in the supercell.<sup>78</sup>

(iii) A self-consistent-field (SCF) calculation is performed, with the new set of occupied KS orbitals in the KS-determinant ansatz. The only restriction in the SCF calculation is to keep the  $e$ - $h$  pair in the affected KS orbitals. It should be stressed that the exchange-correlation functional is approximated with an ordinary ground-state GGA for both the ground and excited states.

(iv) The excitation energy is needed to define the diabatic PES and is evaluated as the difference between total energies for the excited- and ground-state configurations, respectively. In order to ensure that the hole is placed in a correctly identified KS orbital in the ground-state  $X_2^\delta/Al(111)^{+\delta}$  configuration, the calculated charge densities of the ground and excited states are analyzed. If the calculated charge density for the excited state should not correspond to the desired excitation [here the neutral  $X_2/Al(111)$  and the charged  $X_2^-/Al^+(111)$  states], all the above-mentioned steps are re-

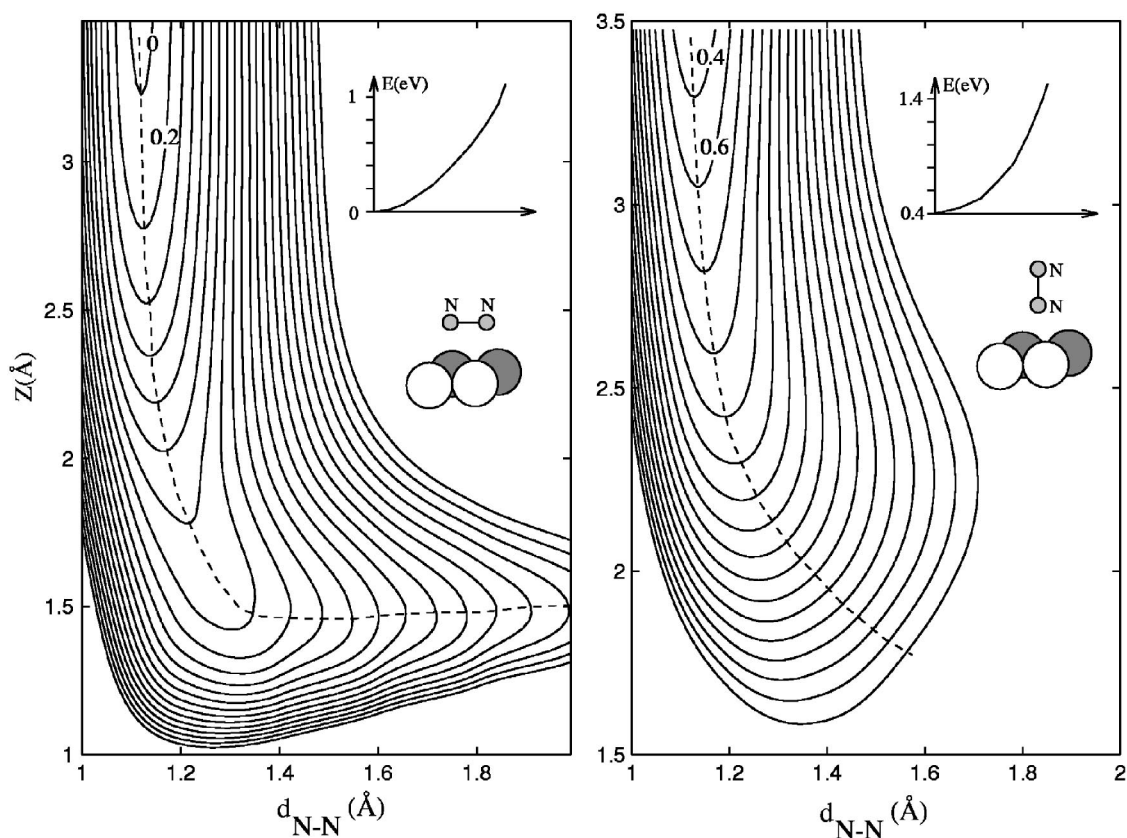


FIG. 15. Cuts through the six-dimensional PES of  $N_2$  as a function of bond length  $d_{N-N}$  and distance  $Z$  above the Al(111) surface above the fcc site in parallel (left) and perpendicular (right) orientations. As insets, the 1D PES along the reaction path (dashed line) are shown.

peated with a new set of  $e-h$  pairs, except for the first adiabatic calculation.

For a more detailed account on how to obtain the diabatic PES using the DFT-based  $\Delta$ SCF method, see the Appendix.

### B. Sticking model

The charge-transfer process is a resonance tunneling of a substrate electron into the LUMO of the molecule. For simplicity, the process is assumed to be irreversible, i.e., there is no back donation of electrons from the molecule to the substrate. This is not only a reasonable approximation<sup>58</sup> but also sufficient here, where the prime target is to give a working mechanism behind the energy dependences of the sticking probability. In contrast to the adiabatic picture, where charge transfer is only a static phenomenon, the diabatic picture of charge transfer includes an essential competition between the time scale for electron tunneling and that for the nuclear motion of the adsorbate. We will use an equation that is based on assumptions about (i) a trajectory approximation [ $\mathbf{r}(t)=z(t)$ ], (ii) tunneling rates that spatially decay exponentially with the distance  $z$  to the surface, and (iii) fractional occupancy of the MO resonance  $n_{X_2^-}(t)$  represented by an ensemble average of the occupation over a macroscopic ensemble of the molecules scattered against the surface.<sup>58</sup> In such a semiclassical trajectory approximation, the time development of the  $X_2^-$  electron population,  $n_{X_2^-}$ , can be described by<sup>58</sup>

$$\frac{d}{dt}n_{X_2^-}(t) = \tau_{res}^{-1}f\{E^A[z(t)]\}[1 - n_{X_2^-}(t)], \quad (1)$$

where  $\tau_{res}^{-1}$  is the resonance filling rate,  $f(E)$  the Fermi-distribution function, and  $E^A[z(t)]$  the surface-affected vertical affinity. The resonance-filling rate is approximated as  $\hbar\tau_{res}^{-1} = 2\Delta_0 \exp(-\alpha_{res}z)$ ,<sup>46,47</sup> where  $\Delta_0$  and  $\alpha_{res}$  are two parameters that describe the resonance width as a function of CM distance. The work-function-affinity energy difference with image correction affects the values of  $\Delta_0$  and  $\alpha_{res}$ . This effect is included in our study by choosing different values for  $\Delta_0$ , reflecting the vertical affinity of the considered molecule.

Our sticking model thus assumes that once a substrate electron has tunneled out to the LUMO of the molecule, there will be no chance for the adsorbate to leave its state of strong chemisorption. Instead, it will reside there until it loses its initial energy and sticks to the surface. This implies that the sticking probability is equal to

$$S_o = n_{X_2^-}(t \rightarrow \infty), \quad (2)$$

including all fragments that stay on the surface and those that are abstracted. Of course the molecule can perform a number of things beyond the first electron transfer, e.g., it can vibrate, rotate, and even be abstracted.<sup>24,26,27,31,47,59</sup> Many of these motions play significant roles in the dynamics of the adsorbate in the inner reaction zone, but they are assumed to

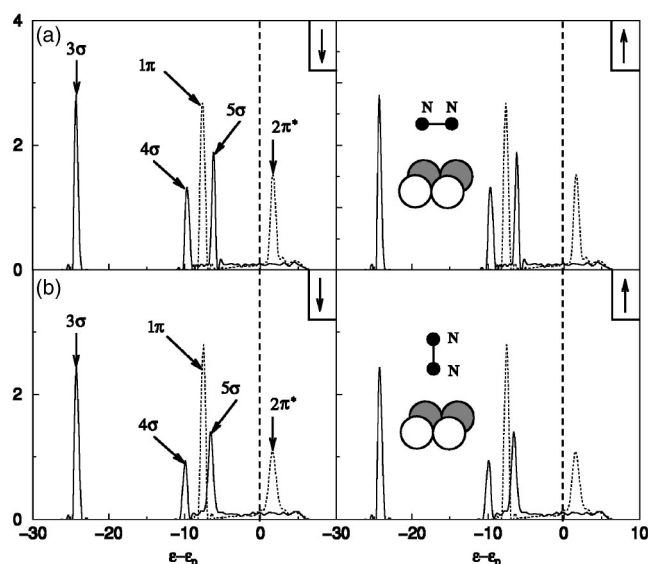


FIG. 16. The local density of states (LDOS) for the  $N_2$  molecule above the fcc site with (a)  $(Z, d_{N-N}, \theta) = (3.0, 1.12 \text{ \AA}, 90^\circ)$  and (b)  $(Z, d_{N-N}, \theta) = (3.0, 1.12 \text{ \AA}, 0^\circ)$ . The left and right panels show the spin-up and -down LDOS's, respectively. The dashed line is the Fermi level.

be events included in the sticking, not to affect the value of the sticking probability.

#### IV. RESULTS AND DISCUSSION

The adiabatic calculations for diatomic molecules on the Al(111) surface highlight many interesting gas-surface-interaction features, such as charge transfer, molecular states, and abstraction. However, they fail to account for the sticking behavior of several of the considered molecules. The physical reason for this is that sticking is a dynamic process, raising questions about nonadiabaticity. In molecule-surface processes with comparable time scales for electron tunneling and nuclear motion of the adsorbate in the chemisorption well, the adiabatic description should be abandoned in favor of a nonadiabatic one.

The choice between the two descriptions is closely related to some specific adsorbate and substrate properties. The present molecular trend study on only one substrate, Al(111), suggests that bond order, electronegativity, kinetic Pauli-repulsion range, and molecular asymmetry are key molecular factors (future studies of trends with respect to substrate properties are likely to include work functions and surface LDOS in their lists of substrate factors). As discussed in the PES section, the bond order sets the scenario, essentially telling how many electrons that can be transferred before the considered molecule loses its molecular identity, i.e., dissociates. It determines the appearance and depth of any chemisorbed molecular state in the PES. The latter three factors are important for the location of the curve crossing. Since at large separations the PES is determined by van der Waals attraction, which should be essentially the same for all molecules, the position of the curve crossing is primarily determined by the electronegativity and the kinetic Pauli repul-

sion range. Here a strong electronegativity allows for an electron transfer far from the surface, whereas a weak kinetic Pauli repulsion allows the considered molecule to come close to the surface. The asymmetry affects the strength of the latter two. In the following, these aspects are further illuminated.

Among the considered homonuclear molecules,  $N_2$  is the one whose electronic structure changes the least upon molecular approach to the surface. This is due to the large HOMO-LUMO gap, unfavorable electronegativity, and high bond order of this molecule. A distinction between adiabatic and diabatic descriptions is then not useful. The calculated adiabatic PES's should fully account for the sticking behavior, i.e., the sticking probability should be zero up to a very high initial translational energy (more than about 2 eV), as has been observed.<sup>22</sup>

For the other homonuclear molecules, i.e.,  $F_2$  and  $O_2$ , however, high electronegativities should favor charge transfer. The calculated LDOS's show that approach of such a molecule to the surface means downshift and filling of the molecular LUMO's. The very high electronegativity of  $F_2$  makes charge transfer energetically allowed far outside the surface, thus allowing electron-hole pair excitation long before  $F_2$  reaches its classical turning point. As a consequence, and as discussed earlier, both the adiabatic and diabatic descriptions yield the same trivial sticking probability of unity for  $F_2$ , for all initial translation energies [Fig. 19(a)], in good agreement with experimental findings.<sup>22</sup> In our sticking model, this is manifested by the curve crossing between  $F_2/Al(111)$  and  $F_2^-/Al(111)^+$  PES's occurring far outside the surface (Fig. 17) and by the weak kinetic Pauli repulsion of  $F_2/Al(111)$ , placing the turning point close to the surface.

For molecules with intermediate electronegativity values, the distinction between adiabatic and diabatic descriptions is clear-cut. In a full account of the sticking behavior in the model case of  $O_2$  on Al(111), the nuclear motion on the entrance-channel diabatic PES should be followed and decay by charge transfer to electron-hole pairs should be allowed for. In a narrow region, the electron tunneling competes with the nuclear motion of the adsorbate with comparable time scales. Incoming molecules with too low initial translation energy might reach their classical turning point, i.e., the initial kinetic energy equals the obtained potential energy in the neutral PES, and bounce back into the gas phase. Molecules with high translation energies reach their classical turning point higher up on the kinetic Pauli-repulsion PES and thus closer to the surface. As the tunneling rate grows exponentially with this distance to the surface, these molecules are more apt for electron transfer from the surface and thus much more likely to enter a region where they can undergo a number of processes, for instance dissociation. In this picture, the experimentally observed sticking behavior of  $O_2$  is accounted for, as illustrated in Fig. 19(a).

The importance of the molecular asymmetry is evident already in the adiabatic PES. As illustrated by Figs. 2, 4, 6, 7, 11, 12, and 15, the PES's depend strongly on the orientation of the molecule in relation to the surface. The molecular asymmetry results in MO asymmetry, both energetically, as illustrated in Figs. 3, 5, 8–10, 13, 14, and 16, and spatially, as, for instance, the  $5\sigma$  MO of CO, which reaches out from

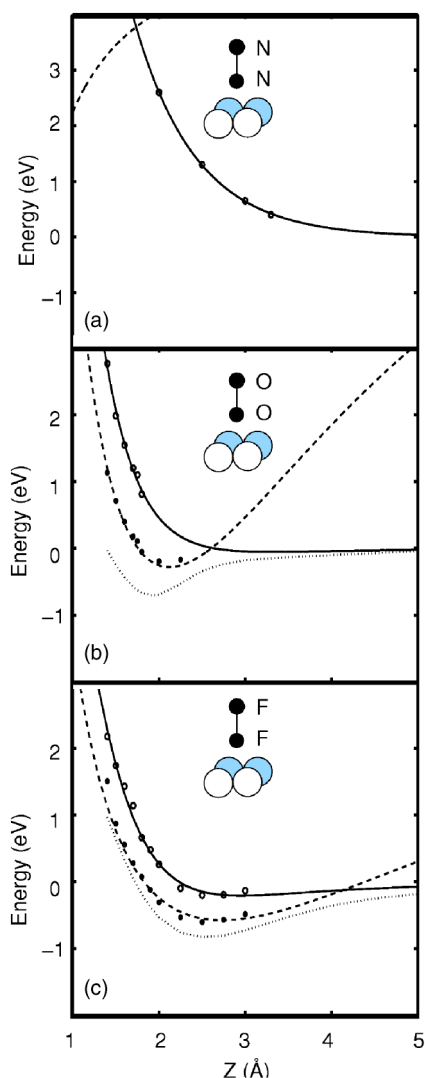


FIG. 17. The adiabatic PES for the  $X_2^{-\delta}/Al^{+\delta}(111)$  (dotted lines) configuration, where  $\delta$  is the charge transferred, and the diabatic PES's for the charged  $X_2^{-\delta}/Al^{+}$  (dashed lines) and the neutral  $X_2/Al(111)$  (solid lines) configurations for (a) the N<sub>2</sub> molecule, (b) the O<sub>2</sub> molecule, and (c) the F<sub>2</sub> molecule in the perpendicular orientation. The distance  $Z$  is defined as the distance between the molecular CM and the first Al layer of the Al(111) surface.

the C atom, giving good overlap with substrate-electron states in a C end-on configuration. In the adiabatic description, such an overlap gives a strongly “avoided curve crossing,” that is, a smooth PES. In the diabatic description, it gives strong charge transfer.

The calculated diabatic PES's for NO and O<sub>2</sub> illustrate that the classical turning point occurs further in for NO than for O<sub>2</sub>. This implies that NO should exhibit a higher sticking probability than O<sub>2</sub> for thermally activated molecules. This is supported both by our sticking-model calculations and by experiment, as illustrated in Fig. 18. One important issue that really affects the sticking for NO is the molecular asymmetry. Our calculated adiabatic PES's for NO illustrate that charge transfer is most efficient for the N end-on orientation, lacking an activation energy in the entrance channel. On the other hand, the O end-on orientation exhibits an energy bar-

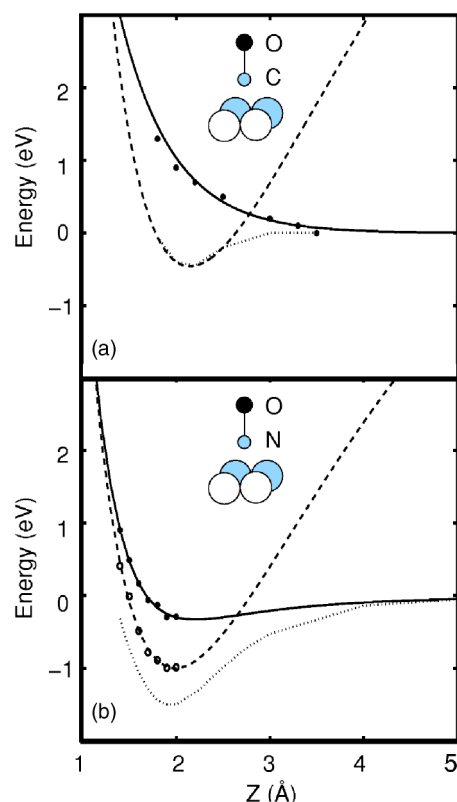


FIG. 18. The adiabatic PES for the  $XY^{-\delta}/Al^{+\delta}(111)$  (dotted lines) configuration, where  $\delta$  is the charge transferred, and the diabatic PES's for the charged  $XY^{-\delta}/Al^{+}$  (dashed lines) and the neutral  $XY/Al(111)$  (solid lines) configurations for (a) the CO molecule in the C end-on orientation, and (b) the NO molecule in the N end-on orientation. The distance  $Z$  is defined as the distance between the molecular CM and the first Al layer of the Al(111) surface.

rier in the exit channel with a height of 0.6 eV. As thermally activated incoming NO molecules are rotating, all the rotational degrees of freedom of the molecule should be taken into account when studying the sticking behavior. It can be argued that the energy barrier for the O end-on orientation is responsible for the experimentally observed saturation of the sticking for larger kinetic energy, i.e., the sticking behavior being less than unity. To fully account for the sticking behavior of NO, a dynamics calculation on the multidimensional PES's is required, which is beyond the scope of the present work. Here, we content ourselves by giving qualitative trends of the observed sticking behavior.

The same asymmetry argument explains the difference in sticking behaviors of CO and N<sub>2</sub>.

In comparing the heteronuclear and thus asymmetric molecules NO and CO, the argument about the effect of electronegativity can be used. It says that NO is more electronegative than CO and then should exhibit a much higher sticking probability than CO [Fig. 19(b)].

## V. CONCLUSION

The virtues of trend studies of electron structure are demonstrated for adsorption of diatomic molecules, such as F<sub>2</sub>,

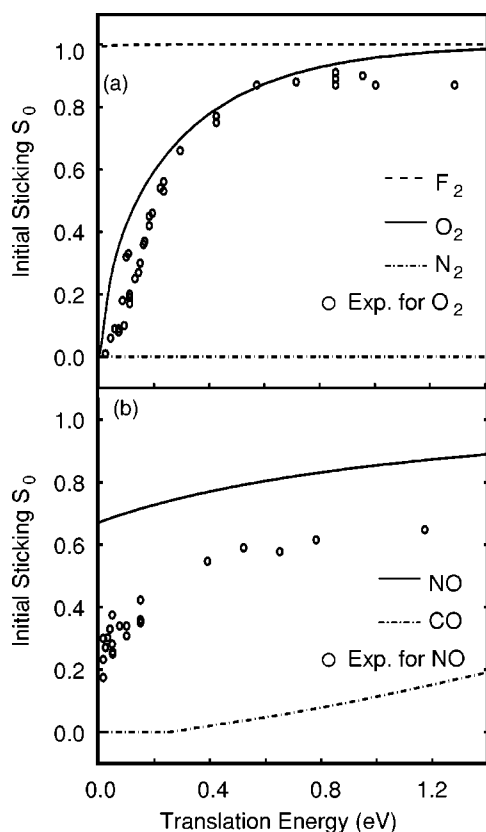


FIG. 19. The calculated initial sticking  $S_0$  as a function of translational energy for (a)  $F_2$ ,  $O_2$ , and  $N_2$ , and (b) NO and CO. The experimental data (Refs. 21 and 31) (unfilled circles) are included for (a)  $O_2$  and (b) NO.

$O_2$ , NO, CO, and  $N_2$ , on the Al(111) surface. These molecules show varying electronegativities, bond orders, Pauli repulsions, and degrees of asymmetry. The analysis is made with the help of DFT, by which both adiabatic and excited-state PES's and LDOS's are calculated. This results in a conceptual picture for molecular chemisorption on a simple *sp*-band metal like Al(111). The study also provides a diabatic description that accounts for dynamic charge transfer and nonadiabatic processes and electron-hole-pair excitation in a way that qualitatively describes the experimentally measured sticking behaviors.

Charge transfer from electronic states at the surface to the LUMO of the adsorbate is identified as the key process in the chemisorption process. This gives a competition between two dynamic processes, electron tunneling and molecular motion close to the surface, and this competition is decisive for the sticking behavior. It relates to several factors where the electronegativity is the key measure to decide between adiabatic and diabatic descriptions (in the general case, the electronegativity should be compared with the work function of the substrate). For both high- and low-electronegativity molecules, an adiabatic description is sufficient to account for the sticking behavior. In the former case, which applies to  $F_2$ , charge transfer can occur far outside the surface, which makes the electron-transfer process able to act for a long time compared to the time for the nuclear motion. In the other case, which applies to  $N_2$ , the low electronegativity makes charge transfer inactive.

For molecules with intermediate electronegativities, i.e.,  $O_2$  and NO, on the other hand, the time scales for the electronic and nuclear processes are comparable in the region of the curve crossing point, indicating efficient nonadiabatic effects. Here, it is concluded that a diabatic account describes the sticking behavior correctly. The one-dimensional model that we use contains the key ingredients. A complete account of the sticking behaviors requires a six-dimensional study, however, which is beyond the scope of this article.

At a finer level, the molecular asymmetry, as in the cases of NO and CO, also affects the sticking. Here asymmetric frontier MO's can overlap more strongly with electronic states of the surface, making charge transfer more active and thus enhancing the sticking probability compared to the corresponding homonuclear isoelectronic molecule, i.e.,  $N_2$  in the case of CO. Although it is less clear-cut, a similar mechanism applies to NO when compared to  $O_2$ .

For molecular chemisorption, a conceptual picture based on bond order and molecular asymmetry comes out as a result of our adiabatic calculations. The well depth of the molecularly chemisorbed states increases with decreasing bond order. CO and  $N_2$  show shallow wells, as they have low electronegativity and high bond orders. Upon molecular approach to the surface, molecular asymmetry affects both ordering between the MO's (for instance, the  $\pi$  and  $\sigma$  MO's have their energies reversed in the heteronuclear molecules compared to the homonuclear ones) and shifts of the MO energy levels (for heteronuclear molecules, such as NO and CO, the MO's of  $\sigma$  type are shifted most, even to the extent that the ordering resembles that of homonuclear molecules in the molecular chemisorption states), giving the heteronuclear molecules a stronger bond to the surface, when properly oriented.

## ACKNOWLEDGMENTS

We thank I. Zoric for fruitful discussions. The work has been supported by the Swedish Science Council and the Swedish Foundation for Strategic Research (SSF) via Materials Consortia No. 9 and ATOMICS, which are gratefully acknowledged.

## APPENDIX

Here the diabatic PES method is illuminated in slightly greater detail. Our first focus will be on the  $O_2$ /Al(111) system. The calculated ground-state LDOS's (Fig. 5) show a continuous filling of the  $2\pi^*$  LUMO resonance of the  $O_2$  molecule upon its approach to the surface, both for parallel and perpendicular orientations. In the latter case, up to two electrons are transferred before the molecule can reach the molecularly chemisorbed state. The adiabatic ground state can thus be assigned an electronic configuration of  $O_2^{-\delta}/Al^{+\delta}(111)$ , where  $\delta$  is a number between 0 and 2, in a large part of our studied range.

The diabatic PES's of particular interest for the sticking model are the neutral  $O_2$ /Al(111) and the charged  $O_2^-/Al^+(111)$  configurations. The additional charge-transfer configuration involved,  $O_2^{-2}/Al^{+2}(111)$ , is not considered

explicitly in our simple sticking model. However, so is the ground-state configuration in the perpendicular orientation close to the Al(111) surface, as its molecularly adsorbed state gives the bottom of the potential well of the diabatic PES for this orientation (Fig. 4).

The electronically excited configurations we obtain by first doing the adiabatic calculation for  $O_2^{-\delta}/Al^{+\delta}(111)$  and then introduce holes into the antibonding  $\pi^*$  LUMO of  $O_2$ , two for the neutral  $O_2/Al(111)$  and one for the charged  $O_2^-/Al^+(111)$  state, respectively. This procedure can be performed for molecule-surface separations  $Z$ , for which the  $\pi^*$  LUMO of the  $O_2$  molecule is completely filled. As  $Z$  is increased, the LUMO resonance successively loses electrons, and beyond a certain  $Z$  value the partial filling corresponds to

less than one electron, a situation that is not well suited for the  $\Delta$ SCF method. Hence, in practice, the diabatic PES's are obtained by the  $\Delta$ SCF method close to the surface and then matched to asymptotic PES's for larger separations, namely the calculated adiabatic PES for the neutral  $O_2/Al(111)$  state and an image potential<sup>60</sup> for the charged  $O_2^-/Al^+(111)$  state has an image potential,<sup>60</sup> accounting for surface and molecule by work function and vertical affinity, respectively.

The same method is applied to the calculation of the diabatic PES's for CO, NO, and  $F_2$ , with only one minor difference for the latter molecule, where the LUMO is the  $\sigma^*$  MO, not the  $\pi^*$  MO. The results of these calculations are presented in Figs. 17 and 18. For  $N_2$ , on the other hand, the diabatic PES is the same as the adiabatic one.

- <sup>1</sup>G. Ertl and J. Küppers, *Low Energy Electrons and Surface Chemistry*, 2nd ed. (VCH, Weinheim, 1985).
- <sup>2</sup>T. A. Delchar and G. Ehrlich, *J. Chem. Phys.* **42**, 2686 (1965).
- <sup>3</sup>D. L. Adams and L. H. Germer, *Surf. Sci.* **27**, 21 (1971).
- <sup>4</sup>S. P. Singh-Boparai, M. Bowker, and D. A. King, *Surf. Sci.* **53**, 55 (1975).
- <sup>5</sup>G. Brodén, G. Gafner, and H. P. Bonzel, *Appl. Phys.* **13**, 333 (1977).
- <sup>6</sup>F. Bozso, G. Ertl, M. Grunze, and M. Weiss, *J. Catal.* **49**, 18 (1977).
- <sup>7</sup>G. Kneringer and F. P. Netzer, *Surf. Sci.* **49**, 125 (1975).
- <sup>8</sup>R. Ducros and R. P. Merrill, *Surf. Sci.* **55**, 227 (1976).
- <sup>9</sup>P. J. Feibelman, *Phys. Rev. Lett.* **67**, 461 (1991).
- <sup>10</sup>G. R. Darling and S. Holloway, *Rep. Prog. Phys.* **58**, 1595 (1995).
- <sup>11</sup>B. Hammer, M. Scheffler, K. W. Jacobsen, and J. K. Nørskov, *Phys. Rev. Lett.* **73**, 1400 (1994).
- <sup>12</sup>J. A. White, D. M. Bird, M. C. Payne, and I. Stich, *Phys. Rev. Lett.* **73**, 1404 (1994).
- <sup>13</sup>B. Hammer, K. W. Jacobsen, and J. K. Nørskov, *Phys. Rev. Lett.* **69**, 1971 (1992).
- <sup>14</sup>B. Hammer, K. W. Jacobsen, and J. K. Nørskov, *Phys. Rev. Lett.* **70**, 3971 (1993).
- <sup>15</sup>S. Wilke, M. H. Cohen, and M. Scheffler, *Phys. Rev. Lett.* **77**, 1560 (1996).
- <sup>16</sup>A. Gross, B. Hammer, M. Scheffler, and W. Brenig, *Phys. Rev. Lett.* **73**, 3121 (1994).
- <sup>17</sup>A. Gross, *Surf. Sci.* **363**, 1 (1996).
- <sup>18</sup>G. R. Darling and S. Holloway, *Surf. Sci.* **304**, L461 (1994).
- <sup>19</sup>J. Dai and J. C. Light, *J. Chem. Phys.* **107**, 1676 (1994).
- <sup>20</sup>G. P. Brivio and M. I. Trioni, *Rev. Mod. Phys.* **71**, 231 (1999).
- <sup>21</sup>L. Österlund, I. Zoric, and B. Kasemo, *Phys. Rev. B* **55**, 15 452 (1997).
- <sup>22</sup>I. Zoric and H. Ternow (private communications).
- <sup>23</sup>M. Binetti, O. Weiß, E. Hasselbrink, A. J. Komrowski, and A. C. Kummel, *Faraday Discuss.* **117**, 313 (2000).
- <sup>24</sup>A. J. Komrowski, J. Z. Sexton, A. C. Kummel, M. Binetti, O. Weisse, and E. Hasselbrink, *Phys. Rev. Lett.* **87**, 246103 (2001).
- <sup>25</sup>K. W. Kolasinski, *Surface Science, Fundamentals of Catalysis and Nanoscience* (John Wiley & Sons, Ltd., 2002), p. 108 ff.
- <sup>26</sup>Y. Yourdshahyan, B. Razaznejad, and B. I. Lundqvist, *Solid State Commun.* **117**, 531 (2001).
- <sup>27</sup>Y. Yourdshahyan, B. Razaznejad, and B. I. Lundqvist, *Phys. Rev. B* **65**, 075416 (2002).
- <sup>28</sup>T. Sasaki and T. Ohno, *Comput. Mater. Sci.* **14**, 8 (1999).
- <sup>29</sup>T. Sasaki and T. Ohno, *Phys. Rev. B* **60**, 7824 (1999).
- <sup>30</sup>K. Honkala and K. Laasonen, *Phys. Rev. Lett.* **84**, 705 (2000).
- <sup>31</sup>A. J. Komrowski, H. Ternow, B. Razaznejad, B. Berenbak, J. Z. Sexton, I. Zoric, B. Kasemo, B. I. Lundqvist, S. Stolte, A. W. Kleyn, and A. C. Kummel, *J. Chem. Phys.* **117**, 8185 (2002).
- <sup>32</sup>L. Vattuone, M. Rocca, C. Boragno, and U. Valbusa, *J. Chem. Phys.* **101**, 713 (1994).
- <sup>33</sup>A. Raukema, D. A. Butler, F. M. A. Box, and A. W. Kleyn, *Surf. Sci.* **347**, 151 (1996).
- <sup>34</sup>P. A. Gravil, D. M. Bird, and J. A. White, *Phys. Rev. Lett.* **77**, 3933 (1996).
- <sup>35</sup>G. D. Billing, *J. Chem. Phys.* **112**, 335 (2000).
- <sup>36</sup>G. P. Brivio, T. B. Grimley, and M. I. Trioni, *J. Chem. Phys.* **114**, 8583 (2001).
- <sup>37</sup>J. K. Nørskov and B. I. Lundqvist, *Surf. Sci.* **89**, 251 (1979).
- <sup>38</sup>L. C. Ciacchi and M. C. Payne, *Phys. Rev. Lett.* **92**, 176104 (2004).
- <sup>39</sup>A. Hellman, B. Razaznejad, Y. Yourdshahyan, H. Ternow, I. Zoric, and B. I. Lundqvist, *Surf. Sci.* **532–535**, 126 (2003).
- <sup>40</sup>T. F. O'Malley, *Adv. At. Mol. Phys.* **7**, 223 (1971).
- <sup>41</sup>G. Katz, Y. Zeiri, and R. Kosloff, *Surf. Sci.* **425**, 1 (1999).
- <sup>42</sup>M. Binetti, O. Weisse, E. Hasselbrink, G. Katz, Y. Zeiri, and R. Kosloff, *Chem. Phys. Lett.* **373**, 266 (2003).
- <sup>43</sup>G. Katz, R. Kosloff, and Y. Zeiri, *J. Chem. Phys.* **120**, 3931 (2004).
- <sup>44</sup>J. Behler, B. Delley, S. Lorenz, K. Reuter, and M. Scheffler, *Phys. Rev. Lett.* **94**, 036104 (2005).
- <sup>45</sup>J. K. Nørskov, D. M. News, and B. I. Lundqvist, *Surf. Sci.* **80**, 179 (1979).
- <sup>46</sup>L. Hellberg, J. Strömquist, B. Kasemo, and B. I. Lundqvist, *Phys. Rev. Lett.* **74**, 4742 (1995).
- <sup>47</sup>J. Strömquist, L. Hellberg, B. Kasemo, and B. I. Lundqvist, *Surf. Sci.* **435**, 352 (1996).
- <sup>48</sup>G. Blyholder, *J. Phys. Chem.* **68**, 2772 (1964).
- <sup>49</sup>B. Hammer, L. B. Hansen, and J. K. Nørskov, *Phys. Rev. B* **59**, 7413 (1999); S. R. Bahn and K. W. Jacobsen, *Comput. Sci. Eng.* **4**, No. 3, 56 (2002). The DACAPO code can be downloaded at <http://www.fysik.dtu.dk/campos>.



- <sup>50</sup>J. P. Perdew, J. A. Chevary, S. H. Vosko, K. A. Jackson, M. R. Pederson, D. J. Singh, and C. Fiolhais, *Phys. Rev. B* **46**, 6671 (1992).
- <sup>51</sup>J. P. Perdew, in *Electronic Structure of Solids '91*, edited by P. Ziesche and H. Eschrig (Akademie Verlag, Berlin, 1991), Vol. 11.
- <sup>52</sup>J. P. Perdew, K. Burke, and M. Ernzerhof, *Phys. Rev. Lett.* **77**, 3865 (1996).
- <sup>53</sup>L. Bengtsson, *Phys. Rev. B* **59**, 12 301 (1999).
- <sup>54</sup>C. Corriol, G. R. Darling, and S. Holloway, *Surf. Sci.* **532**, 198 (2003).
- <sup>55</sup>O. Weiße, C. Wesenberg, M. Binetti, E. Hasselbrink, C. Corriol, G. R. Darling, and S. Holloway, *J. Chem. Phys.* **118**, 8010 (2003).
- <sup>56</sup>A. Hellman, B. Razaznejad, and B. I. Lundqvist, *J. Chem. Phys.* **120**, 4593 (2004).
- <sup>57</sup>J. C. Slater, *Phys. Rev.* **32**, 339 (1928).
- <sup>58</sup>D. C. Langreth and P. Nordlander, *Phys. Rev. B* **43**, 2541 (1991).
- <sup>59</sup>O. Citri, R. Baer, and R. Kosloff, *Surf. Sci.* **351**, 24 (1996).
- <sup>60</sup>P. J. Jennings, R. O. Jones, and M. Weinert, *Phys. Rev. B* **37**, 6113 (1988).
- <sup>61</sup>C. T. Rettner and C. B. Mullins, *J. Chem. Phys.* **94**, 1626 (1991).
- <sup>62</sup>C. T. Rettner, L. A. DeLouise, and D. J. Auerbach, *J. Chem. Phys.* **85**, 1131 (1986).
- <sup>63</sup>R. W. Verhoef, D. Kelly, and W. H. Weinberg, *Surf. Sci.* **306**, L513 (1994).
- <sup>64</sup>C. B. Mullins, Y. Wang, and W. H. Weinberg, *J. Vac. Sci. Technol. A* **7**, 2125 (1989).
- <sup>65</sup>M. E. M. Spruit, E. W. Kuipers, F. H. Guezebhoek, and A. W. Kleyn, *Surf. Sci.* **215**, 421 (1989).
- <sup>66</sup>D. E. Eastman and J. E. Demuth, *Jpn. J. Appl. Phys., Suppl.* **2**, 827 (1974).
- <sup>67</sup>H. Conrad, G. Ertl, J. Küppers, and E. E. Latta, *Surf. Sci.* **50**, 296 (1975).
- <sup>68</sup>R. A. Marbrow and R. M. Lambert, *Surf. Sci.* **61**, 317 (1976).
- <sup>69</sup>P. J. Goddard, J. West, and R. M. Lambert, *Surf. Sci.* **71**, 447 (1978).
- <sup>70</sup>J. F. Wendelken, *Appl. Surf. Sci.* **11**, 172 (1982).
- <sup>71</sup>M. Kiskinova, G. Pirug, and H. P. Bonzel, *Surf. Sci.* **136**, 285 (1984).
- <sup>72</sup>H. Conrad, G. Ertl, J. Küppers, and E. E. Latta, *Surf. Sci.* **6**, 1235 (1977).
- <sup>73</sup>B. Hammer, Y. Morikawa, and J. K. Nørskov, *Phys. Rev. Lett.* **76**, 2141 (1996).
- <sup>74</sup>C. T. Rettner and H. Stein, *Phys. Rev. Lett.* **59**, 2768 (1987).
- <sup>75</sup>C. R. Arumaiyanayagam and R. J. Madix, *Prog. Surf. Sci.* **38**, 1 (1991).
- <sup>76</sup>G. Ehrlich, *Activated Chemisorption*, in *Chemistry and Physics of Solid Surfaces VII*, edited by R. Vanselow and R. F. Howe (Springer, New York, 1988), Vol. 10, p. 1.
- <sup>77</sup>Experimental data in the literature might cause some confusion on sticking behaviors, as they show few general trends but rather unsystematic variations. For instance, the thermal sticking  $S_0$  for  $N_2$  is reported to be very low ( $\sim 0.004$ ) on  $W(110)^2$  but large ( $\sim 0.70$ ) on the (310) and (320) faces.<sup>3,4</sup> On Fe it differs by three orders of magnitude between different surfaces, with the lowest values ( $\sim 10^{-7}$ ) for the (110) (Ref. 5) and (100) faces<sup>6</sup> and the largest one ( $\sim 10^{-4}$ ) for the (111) face.<sup>6</sup> For  $O_2$  on Pt, it is measured to be  $\sim 10^{-4}$  and  $\sim 0.4$  on the (100) (Ref. 7) and (111) surfaces,<sup>8</sup> respectively.
- <sup>78</sup>In a general adiabatic DFT calculation on an extended system, the LUMO resonance of the molecule is filled continuously upon molecule approach to the surface. Our extended-DFT excitation-method,<sup>56</sup> however, utilizes the supercell to get discrete levels with integer occupancy and at this point does not account for any introduction of fractional numbers of  $e-h$  pairs. Thus the electronically excited configurations can be obtained only for certain adsorbate-surface separations, where an integer number of electrons are transferred to the adsorption-modified LUMO of the molecule and where the adsorbate and substrate do not share the “transferred” electron among their electronic states.